

AD-764 721

TRANSIENT SIGNAL PROPAGATION IN LOSSY  
PLASMAS

Ronald L. Fante, et al

Air Force Cambridge Research Laboratories  
L. G. Hanscom Field, Massachusetts

25 April 1973

DISTRIBUTED BY:

**NTIS**

National Technical Information Service  
U. S. DEPARTMENT OF COMMERCE  
5285 Port Royal Road, Springfield Va. 22151

AD 764721

AFCRL-TR-73-0277

25 APRIL 1973

PHYSICAL SCIENCES RESEARCH PAPERS, NO. 546



**AIR FORCE CAMBRIDGE RESEARCH LABORATORIES**

L. G. HANSCOM FIELD, BEDFORD, MASSACHUSETTS

## **Transient Signal Propagation in Lossy Plasmas**

**RONALD L. FANTE**

**RICHARD L. TAYLOR**

By  
NATIONAL TECHNICAL  
INFORMATION SERVICE

Approved for public release; distribution unlimited.

**AIR FORCE SYSTEMS COMMAND**

**United States Air Force**



Unclassified  
Security Classification

DOCUMENT CONTROL DATA - R'D		
(Security classification of title, body of abstract and indexing annotation must be entered when the overall report is classified)		
1. ORIGINATING ACTIVITY (Corporate author) Air Force Cambridge Research Laboratories (LZP) L.G. Hanscom Field Bedford, Massachusetts 01730		2a. REPORT SECURITY CLASSIFICATION Unclassified
		2b. GROUP
3. REPORT TITLE  TRANSIENT SIGNAL PROPAGATION IN LOSSY PLASMAS		
4. DESCRIPTIVE NOTES (Type of report and inclusive dates) Scientific. Interim.		
5. AUTHOR(S) (First name, middle initial, last name) Ronald L. Fante Richard L. Taylor		
6. REPORT DATE 25 April 1973	7a. TOTAL NO. OF PAGES 38	7b. NO. OF REFS 11
8a. CONTRACT OR GRANT NO.		9a. ORIGINATOR'S REPORT NUMBER(S) AFCRL-TR-73-0277
b. PROJECT, TASK, WORK UNIT NOS. 5635-04-01		
c. DOD ELEMENT 61102F		
d. DOD SUBELEMENT 681305	9b. OTHER REPORT NO(S) (Any other numbers that may be assigned this report) PSRP No. 546	
10. DISTRIBUTION STATEMENT  Approved for public release; distribution unlimited.		
11. SUPPLEMENTARY NOTES  TECH, OTHER		12. SPONSORING MILITARY ACTIVITY Air Force Cambridge Research Laboratories (LZP) L.G. Hanscom Field Bedford, Massachusetts 01730
13. ABSTRACT Using contour integration techniques, we have calculated the transient response of a lossy homogeneous isotropic plasma to a unit step and a step-carrier sine wave. We have found that in the presence of losses the temporal step function response within the plasma does not approach zero for large time as for the collisionless case, but rather approaches unity. The rate at which the transient approaches the asymptotic value of unity is strongly dependent on the losses, being quite rapid for large losses and exceedingly slow for very small losses. This result has an important impact on the propagation of EMP through the plasma sheath around a reentry vehicle, and through the ionized region near a low altitude nuclear fireball.		

DD FORM 1473  
1 NOV 63

Unclassified  
Security Classification

~~Unclassified~~  
~~Security Classification~~

14.	KEY WORDS.	LINK A		LINK B		LINK C	
		ROLE	WT	ROLE	WT	ROLE	WT
	Transient propagation Plasmas						

~~Unclassified~~  
~~Security Classification~~

## Abstract

Using contour integration techniques, we have calculated the transient response of a lossy homogeneous isotropic plasma to a unit step and a step-carrier sine wave. We have found that in the presence of losses the temporal step-function response within the plasma does not approach zero for large time as for the collisionless case, but rather approaches unity. The rate at which the transient approaches the asymptotic value of unity is strongly dependent on the losses, being quite rapid for large losses and exceedingly slow for very small losses. This result has an important impact on the propagation of EMP through the plasma sheath around a reentry vehicle, and through the ionized region near a low altitude nuclear fireball.

## Contents

1. INTRODUCTION	1
2. BRANCH POINTS AND BRANCH-CUTS	2
3. NUMERICAL RESULTS	6
3.1 Step-Carrier Sine Wave	6
3.2 Step-Function	13
4. DISCUSSION	16
REFERENCES	21
APPENDIX A	23
APPENDIX B	25
APPENDIX C	27
APPENDIX D	29

## Illustrations

1. Branch-Cuts for the Functions (a) $\gamma_1$ , (b) $\gamma_2$ , (c) $\gamma_3$ , (d) $\gamma_4$	3
2. Branch-Cuts for the Function $\gamma$ When $\nu_c < 2\omega_p$	4
3. Branch-Cuts for the Function $\gamma$ When $\nu_c > 2\omega_p$	5

Preceding page blank

## Illustrations

4. Deformed Contour Integration for the Case When $\nu_c < 2\omega_p$	6
5. Transient Response to Step-Carrier Sine Wave for $\omega_0 x/c = 1$ and $\omega_p/\omega_0 = 2$	7
6. Transient Response to Step-Carrier Sine Wave for $\omega_0 x/c = 5$ and $\omega_p/\omega_0 = 2$	8
7. Transient Response to Step-Carrier Sine Wave for $\omega_0 x/c = 10$ and $\omega_p/\omega_0 = 2$	8
8. Transient Response to Step-Carrier Sine Wave for $\nu_c/\omega_p = 0.5$ and $\omega_p/\omega_0 = 2$	10
9. Transient Response to Step-Carrier Sine Wave for $\nu_c/\omega_p = 1.0$ and $\omega_p/\omega_0 = 2$	10
10. Transient Response to Step-Carrier Sine Wave for $\omega_0 x/c = 0.5$ and $\omega_p/\omega_0 = 4$	11
11. Transient Response to Step-Carrier Sine Wave for $\omega_0 x/c = 2.5$ and $\omega_p/\omega_0 = 4$	11
12. Transient Response to Step-Carrier Sine Wave for $\omega_0 x/c = 5$ and $\omega_p/\omega_0 = 4$	12
13. Transient Response to Step-Carrier Sine Wave for $\omega_0 x/c = 5$ and $\omega_p/\omega_0 = 0.7$	12
14. Transient Response to Unit Step for $\omega_p x/c = 1$	14
15. Transient Response to Unit Step for $\omega_p x/c = 5$	14
16. Transient Response to Unit Step for $\omega_p x/c = 10$	15
17. Transient Response to Unit Step for $\nu_c/\omega_p = 1$	15
18. Response to a $10^{-6}$ sec Square Pulse for (a) $\nu_c = 0$ , $\omega_p = 1.5 \times 10^{10}$ and (b) $\nu_c = \omega_p = 1.5 \times 10^{10}$	19
19. Transient Response of a Conductor or Lossy Dielectric to a Unit Step	19

## Tables

1. Comparison of Exact Results for the Transient E-Field With the Approximation of Eq. (16) for $\nu_c/\omega_p = 1$	17
2. Comparison of Exact Results for the Transient E-Field With the Approximation of Eq. (16) for $\nu_c/\omega_p = 0.1$	17

## Transient Signal Propagation in Lossy Plasmas

### I. INTRODUCTION

There has been a great deal of research done (Haskell and Case, 1966a, b, 1967; Knop and Cohn, 1963; Knop, 1965; Lighthill, 1965; Felsen, 1969; Antonucci, 1972) on the transient propagation of electromagnetic signals through lossless plasmas, and the results are quite appropriate for the calculation of EMP through the undisturbed ionosphere. For transmission of EMP through the plasma surrounding a reentry vehicle or through the ionized region near a low altitude nuclear fireball, however, the theory is quite inadequate since here the effect of collisional absorption on the transient propagation is quite significant. The effect of collisional losses has been considered previously by Field (1971) using the method of characteristics, but unfortunately he does not present results for the transmitted field in the cases of interest to us. In this report, we will therefore extend the previous theories to include the effect of collisional absorption on the propagation of transients in a cold\*, homogeneous isotropic plasma. We shall consider only two types of transient signals: the step-carrier sine wave and the unit step. The transient

---

\* The cold plasma model is approximately valid in those regions near a nuclear burst where the electron temperature is less than  $30,000^{\circ}\text{K}$ . Also, in applying these results to EMP propagation we must be sufficiently far from the fireball to neglect nonlinear effects.

(Received for publication 24 April 1973)



response within the plasma to the unit step is quite important since the response to an arbitrary EMP can always be synthesized as a superposition of the unit step responses.

As a starting point for our investigation we consider the Maxwell equations for the electric field strength  $E$ , and the Langevin equation for the electron velocity  $v$ . If we write  $E$  in terms of the Laplace transform

$$E(x, t) = \int_{\Gamma} \hat{E}(x, p) e^{pt} dp, \quad (1)$$

it is readily shown that for  $x \geq 0$

$$\hat{E}(x, p) = \hat{E}(x=0, p) e^{-\gamma \frac{x}{c}}, \quad (2)$$

where

$$\gamma = \left( \frac{p}{p + \nu} \right)^{1/2} (p^2 + \nu_c p + \omega_p^2)^{1/2}, \quad (3)$$

$\omega_p$  = electron-plasma frequency,

$\nu_c$  = electron - neutral collision frequency.

We have also assumed that  $E(x, t=0)=0$  for all  $x > 0$ . In order to evaluate  $E(x, t)$ , it is necessary to perform the integration along the Bromwich contour  $\Gamma$  in Eq. (1). This may be accomplished either by integrating directly along the Bromwich contour, or by deforming that contour into the left-half  $p$ -plane. This latter choice leads to integrals which rapidly converge, and will therefore be pursued in this report.

## 2. BRANCH POINTS AND BRANCH CUTS

The function  $\gamma$  in Eq. (3) can be written in product form as

$$\gamma = \gamma_1 \gamma_2 \gamma_3 \gamma_4, \quad (4)$$

where  $\gamma_1 = i^{1/2}$ ,  $\gamma_2 = (p + \nu_c)^{-1/2}$ ,  $\gamma_3 = (p - p_1)^{1/2}$ ,  $\gamma_4 = (p - p_2)^{1/2}$ . For  $\nu_c < 2\omega_p$  we have

$$p_{1/2} = -\frac{\nu_c}{2} \pm \left( \omega_p^2 - \nu_c^2/4 \right)^{1/2},$$

while for  $\nu_c > 2\omega_p$  we have

$$p_1 = -\frac{\nu_c}{2} \pm (\nu_c^2/4 - \omega_p^2)^{1/2}.$$

The function  $\gamma_1$  has branch points at  $p = 0$  and  $p = \infty$ . For this function we choose the branch cut shown in Figure 1a. The function  $\gamma_2$  has branch points at  $p = -\nu_c$

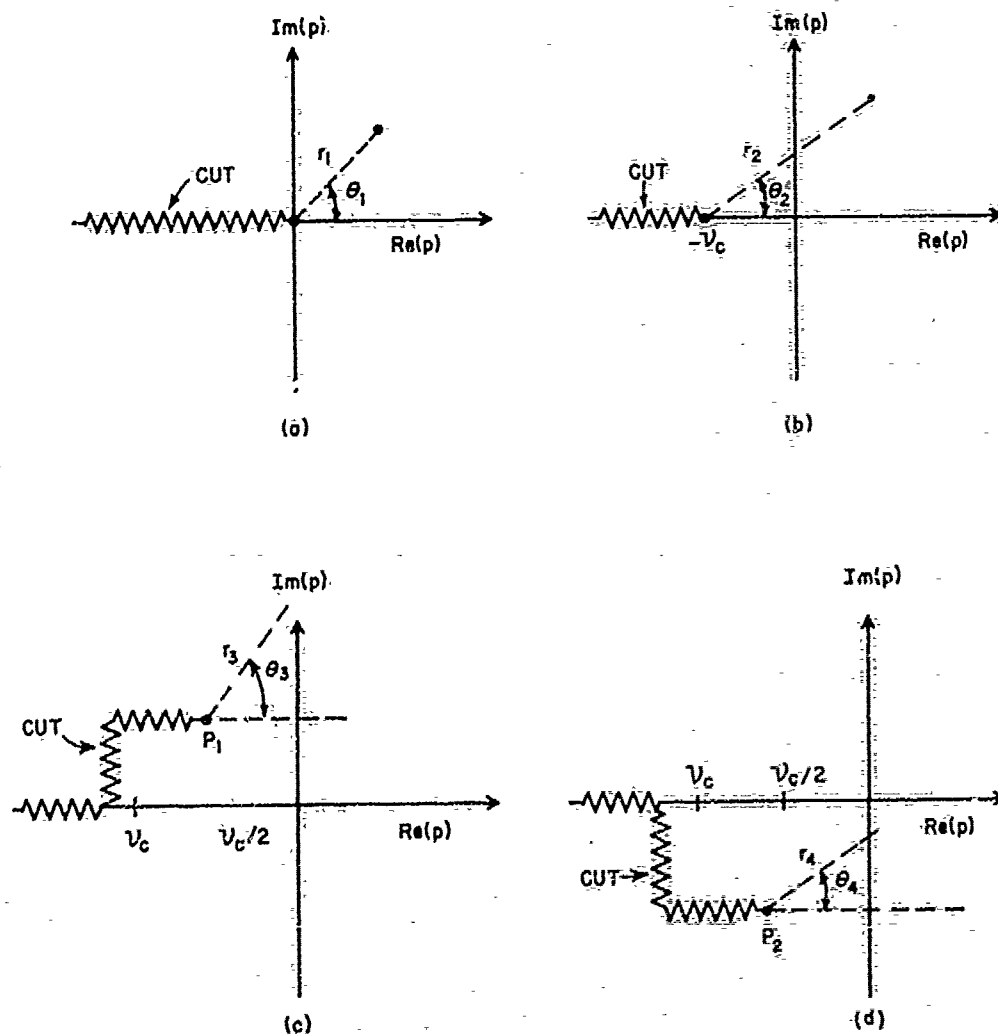


Figure 1. Branch Cuts for the Functions (a)  $\gamma_1$ , (b)  $\gamma_2$ , (c)  $\gamma_3$ , (d)  $\gamma_4$

and  $p = \infty$ , and we choose the branch cut shown in Figure 1b for this quantity. For  $\gamma_c$ , which has branch points at  $p = p_1$  and  $p = \infty$ , we choose the branch cut illustrated in Figure 1c, while for  $\gamma_4$ , which has branch points at  $p = p_2$  and  $p = \infty$ , we choose the branch cut shown in Figure 1d. If we write  $p = r_1 \exp(i\theta_1)$ ,  $(p + \nu_c) = r_2 \exp(i\theta_2)$ ,  $(p - p_1) = r_3 \exp(i\theta_3)$ ,  $(p - p_2) = r_4 \exp(i\theta_4)$ , we can write  $\gamma_1 = \pm r_1^{1/2} \exp(i\theta_1/2)$ ,  $\gamma_2 = \pm r_2^{1/2} \exp(-i\theta_2/2)$ ,  $\gamma_3 = \pm r_3^{1/2} \exp(i\theta_3/2)$  and  $\gamma_4 = \pm r_4^{1/2} \exp(i\theta_4/2)$ . For each of these functions we then choose the Riemann sheet corresponding to the upper sign, so that

$$\gamma = \left( \frac{r_1 r_3 r_4}{r_2} \right)^{1/2} \exp \left[ i \left( \frac{\theta_1 - \theta_2 + \theta_3 + \theta_4}{2} \right) \right], \quad (5)$$

and the branch cuts for the total function  $\gamma = \gamma_1 \gamma_2 \gamma_3 \gamma_4$  are those shown in Figure 2 for  $\nu_c < 2\omega_p$ , and in Figure 3 for  $\nu_c > 2\omega_p$ . The integral in Eq. (1) can now be performed by deforming the Bromwich Contour B in Figure 2 into the

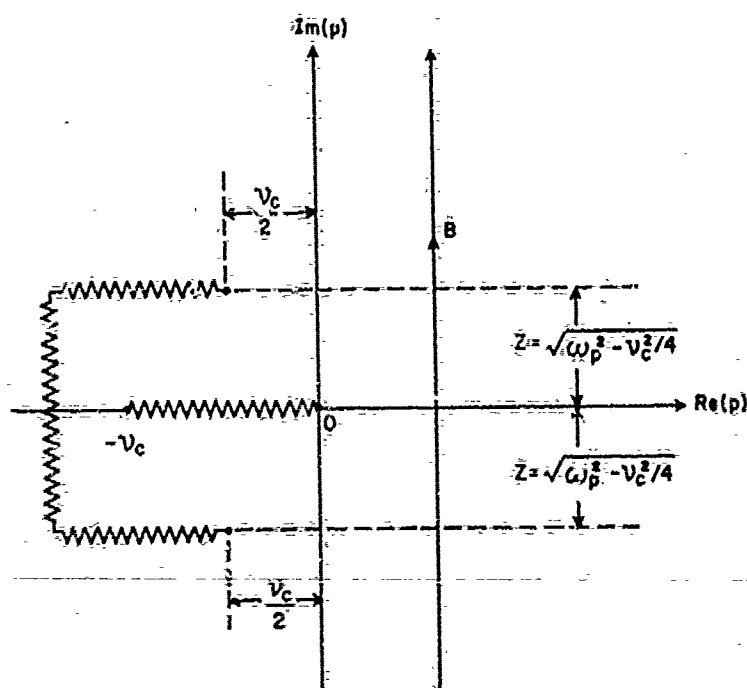


Figure 2. Branch Cuts for the Function  $\gamma$  when  $\nu_c < 2\omega_p$

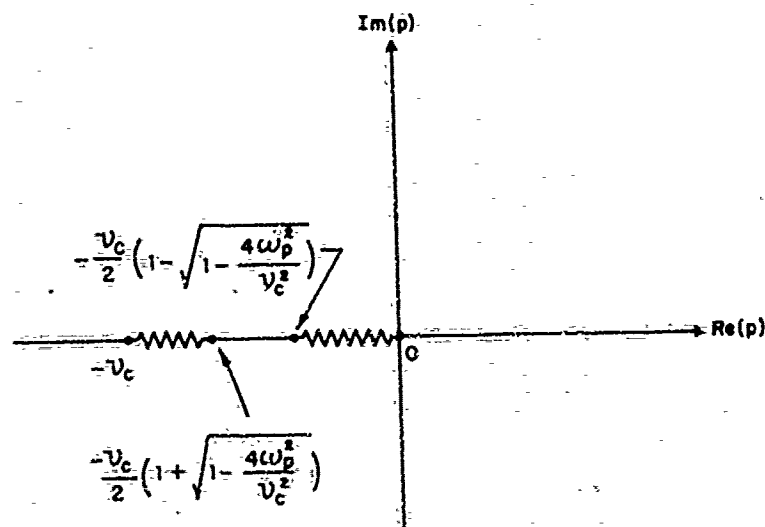


Figure 3. Branch Cuts for the Function  $\gamma$  When  $v_c > 2\omega_p$

left-half  $p$ -plane. If we assume that  $\hat{E}(x=0, p)$  has pole at  $s_0$  and  $s_1$ , then Eq. (1) can be rewritten

$$E(x, t) = \int_{C_1} + \int_{C_2} + \int_{C_3} + \int_{C_4} \hat{E}(x=0, p) e^{(pt - \frac{\gamma x}{c})} dp, \quad (6)$$

where the contours  $C_1$ ,  $C_2$ ,  $C_3$ , and  $C_4$  are shown in Figure 4.

To illustrate how the contour integrals are performed, let us consider the integral along  $C_1$  in Figure 4. At a point A on  $C_1$  we have  $r_1 = \sigma$ ,  $r_2 = v_c - \sigma$ ,  $r_3 = r_4 = (\omega_p^2 - v_c \sigma + \sigma^2)^{1/2}$ , and  $\theta_1 = \pi$ ,  $\theta_2 = 0$ ,  $\theta_3 + \theta_4 = 0$ . At the point B on  $C_1$ ,  $r_1$ ,  $r_2$ ,  $r_3$  and  $r_4$  remain the same but  $\theta_1$  is now  $-\pi$ . Therefore at point A we find upon using these results in Eq. (5) that  $\gamma = i[\sigma/(v_c - \sigma)]^{1/2} (\omega_p^2 + \sigma^2 - v_c \sigma)^{1/2}$ , while at point B,  $\gamma = -i[\sigma/(v_c - \sigma)]^{1/2} (\omega_p^2 + \sigma^2 - v_c \sigma)^{1/2}$ . As a result the integral along contour  $C_1$  can be written as [using the fact that  $p = \sigma \exp(i\pi)$  and  $dp = -d\sigma$ ]

$$\begin{aligned} I_{C_1} &= -\frac{1}{2\pi i} \int_0^{v_c} d\sigma \hat{E}(0, p = -\sigma) e^{-\sigma t} \exp \left[ -i \frac{x}{c} \left( \frac{\sigma}{v_c - \sigma} \right)^{1/2} (\omega_p^2 + \sigma^2 - v_c \sigma)^{1/2} \right] \\ &\quad - \frac{1}{2\pi i} \int_{v_c}^0 d\sigma \hat{E}(0, p = -\sigma) e^{-\sigma t} \exp \left[ i \frac{x}{c} \left( \frac{\sigma}{v_c - \sigma} \right)^{1/2} (\omega_p^2 + \sigma^2 - v_c \sigma)^{1/2} \right] \\ &= -\frac{1}{\pi} \int_0^{v_c} d\sigma \hat{E}(0, -\sigma) e^{-\sigma t} \sin \frac{x}{c} \left[ \left( \frac{\sigma}{v_c - \sigma} \right) (\omega_p^2 + \sigma^2 - v_c \sigma) \right]^{1/2}. \end{aligned} \quad (7)$$

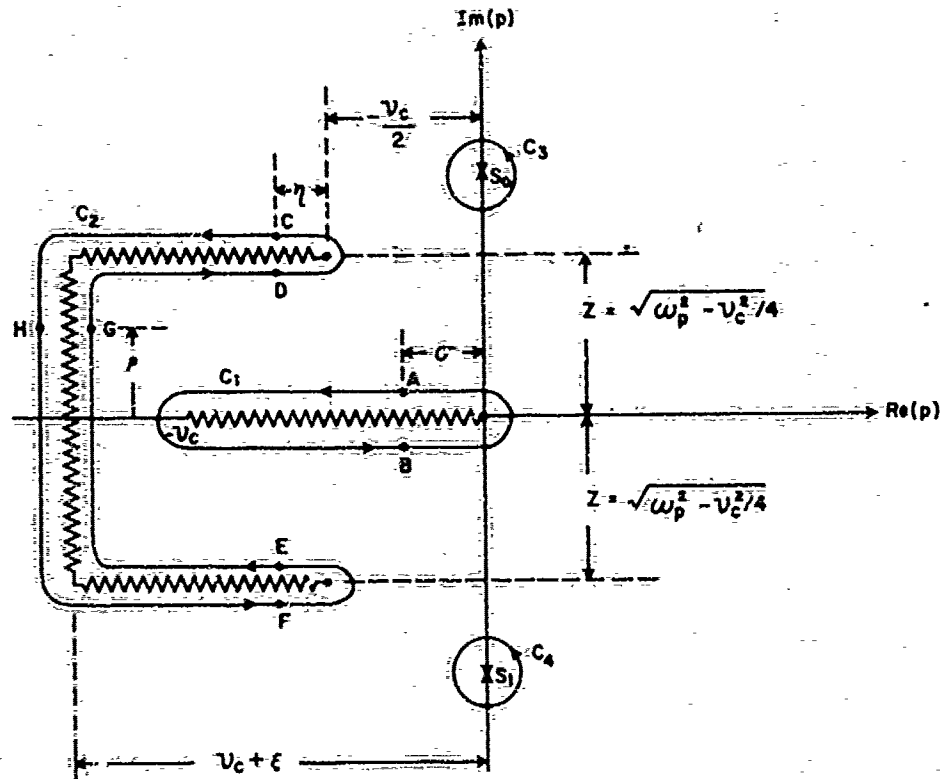


Figure 4. Deformed Contour of Integration for the Case When  $\nu_c < 2\omega_p$

The integral along the contour  $C_2$  is evaluated in the same fashion, while the integration along the contours  $C_3$  and  $C_4$  is trivial. For the interested reader, the details of the integration along  $C_2$  are contained in the Appendix B to this report.

### 3. NUMERICAL RESULTS

### 3.1 Step-Carrier-Sinc-Wave

We first consider the case when  $E(x=0, t)$  is given by

$$E(x=0, t) = u(t) \sin \omega_0 t \quad (8)$$

where  $u(t)$  is the unit step-function. For this case  $\hat{E}(0, p) = \omega_0 / (p^2 + \omega_0^2)$ , so that the poles  $s_0$  and  $s_1$  shown in Figure 4 are  $s_0 = i\omega_0$ ,  $s_1 = -i\omega_0$ . If we define  $\hat{r}_1 = \omega_0$ ,  $\hat{r}_2 = (\omega_0^2 + v_c^2)^{1/2}$ ,  $\hat{r}_3 = [(v_c/2)^2 + (\omega_0 - Z)^2]^{1/2}$ ,  $\hat{r}_4 = [(v_c/2)^2 + (\omega_0 + Z)^2]^{1/2}$  and

$\hat{\theta}_1 = \pi/2$ ,  $\hat{\theta}_2 = \tan^{-1}(\omega_0/\nu_c)$ ,  $\hat{\theta}_3 = \tan^{-1}[2(\omega_0 - Z)/\nu_c]$  and  $\hat{\theta}_4 = \tan^{-1}[2(\omega_0 + Z)/\nu_c]$ , we get

$$\gamma = \Gamma e^{i\Phi} = \left( \frac{\hat{r}_1 \hat{r}_3 \hat{r}_4}{r_2} \right) \exp \frac{i}{2} [\hat{\theta}_1 - \hat{\theta}_2 + \hat{\theta}_3 + \hat{\theta}_4] \quad (9)$$

so that the integral over  $C_3$  and  $C_4$  yields

$$I_{C_3} + I_{C_4} = \exp(-\frac{x}{c} \Gamma \cos \Phi) \sin(\omega_0 t - \Gamma \frac{x}{c} \sin \Phi). \quad (10)$$

Using Eqs. (6), (7), (10) and (A5), we have calculated the time response of the electric field in the plasma for the step-carrier sine wave excitation of Eq. (8). Figure 5 shows the response at  $\frac{\omega_0 x}{c} = 1$  for an overdense plasma ( $\omega_p/\omega_0 = 2$ ) for different values of  $\nu_c$ . We comment that the results for  $\nu_c/\omega_p = 0.01$  are nearly identical with those obtained by Haskell and Case (1966a) for the case  $\nu_c/\omega_p = 0$ . For  $\nu_c/\omega_p = 1$ , however, the response is quite different. This difference is even more apparent for the cases when  $\frac{\omega_0 x}{c} = 5$  and  $\frac{\omega_0 x}{c} = 10$ , which are shown in Figures 6 and 7. For large values of  $\omega_0 x/c$ , even when  $\nu_c/\omega_p = 0.1$ , the transient

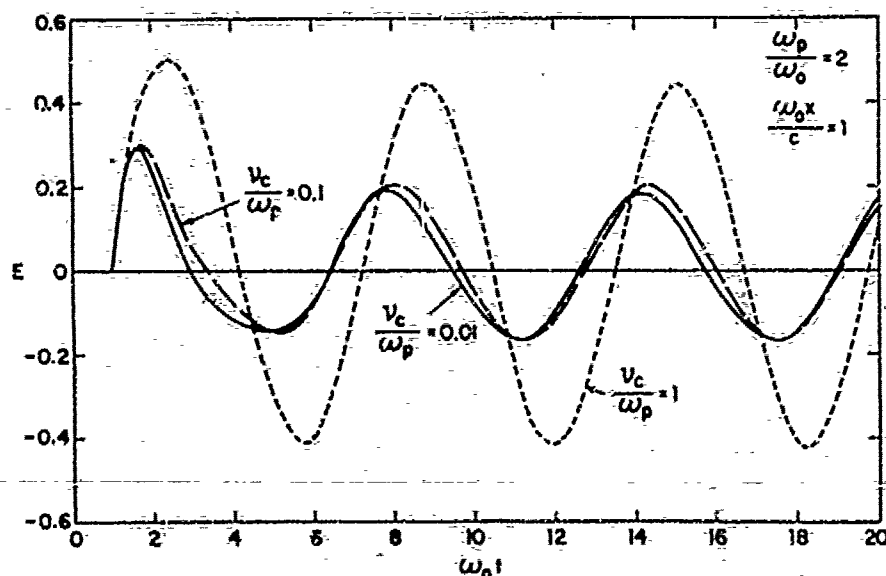


Figure 5. Transient Response to Step-Carrier Sine Wave for  $\omega_0 x/c = 1$  and  $\omega_p/\omega_0 = 2$

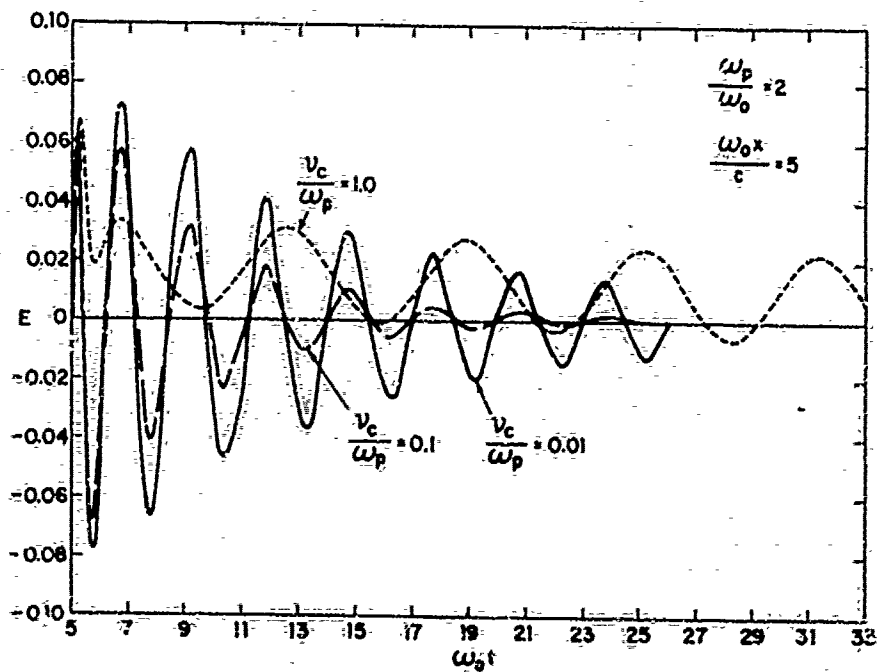


Figure 6. Transient Response to Step-Carrier Sine Wave for  $\omega_0 x/c = 5$  and  $\omega_p/\omega_0 = 2$

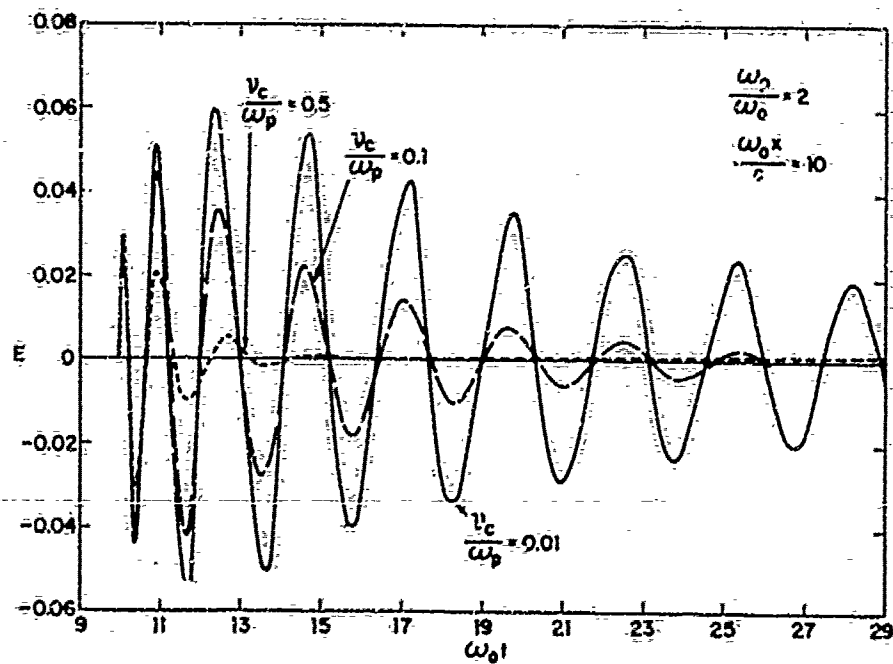


Figure 7. Transient Response to Step-Carrier Sine Wave for  $\omega_0 x/c = 10$  and  $\omega_p/\omega_0 = 2$

response is altered significantly, and for  $\nu_c/\omega_p = 1$  the character of the response is completely different from the collisionless limit. Figures 8 and 9 illustrate how the nature of the transmitted signal changes as the distance into the plasma is varied. We note from Figures 8 and 9 that for large  $\omega_0 x/c$ , there is an oscillation followed by a long wake in which the amplitude of the signal is nearly constant. It is readily shown that in this wake region,  $E(x, t)$  can be approximated\* by (see Appendix B)

$$E(x, t) = \exp\left(-\Gamma \frac{x}{c} \cos \Phi\right) \sin\left(\omega_0 t - \Gamma \frac{x}{c} \sin \Phi\right) + \frac{\omega_p}{2\omega_0 c(\nu_c \pi)^{1/2}} \left(\frac{x}{t^{3/2}}\right) \exp\left(-\frac{\omega_p^2 x^2}{4c^2 \nu_c t}\right). \quad (11)$$

In deriving Eq. (11) we have assumed that  $t \gg x/c$  and that  $\nu_c/\omega_p$  is of order unity. From Eq. (11) we see that for large  $t$  the transient signal consists of a sinusoidal wave at frequency  $\omega_0$  plus a component which eventually decays towards zero as  $t^{-3/2}$ .

Figures 10 through 12 indicate the nature of the response for  $\omega_p/\omega_0 = 4$ . Figure 10 shows the transient response for  $\omega_0 x/c = 0.5$ , where the effect of large values of  $\nu_c$  is to radically alter the signal amplitude. From Figure 11 we see that when  $\omega_0 x/c = 2.5$ , both the amplitude and the character of the transient response are radically changed from the case of zero collision frequency. In fact, the frequency of the oscillation for  $\nu_c/\omega_p = 1$  is quite drastically reduced from the case when  $\nu_c/\omega_p = 0.01$ . Figure 12 illustrates the transient response at  $\omega_0 x/c = 5$ . At this distance, for  $\nu_c/\omega_p = 1$ , there is hardly any oscillation of the transient response, but rather a slow buildup, and then an eventual decay (not shown in the figure) in accordance with the second term in Eq. (11), since the first term in Eq. (11) is quite small for this case.

In Figure 13, we have shown the effect of collisions on propagation in an underdense plasma. Here we note that no interesting or unexpected behavior occurs, and we will not study the underdense case further. In addition, this case has been previously considered by Case and Haskell (1967). We only comment that our results do agree with the previous ones obtained by Haskell and Case (1966a) in the limit  $\nu_c/\omega_p \rightarrow 0$ .

---

\*To check the accuracy of Eq. (11), let us consider the case when  $\nu_c/\omega_p = 1$ ,  $\omega_p/\omega_0 = 2$  and  $\omega_0 L/c = 10$ . If we take a point in the signal wake at  $\omega_0 t = 15$ , we have from Eq. (11) that  $E = 2.54 \times 10^{-3}$ , while the exact calculation (see Figure 9) gives  $E = 2.51 \times 10^{-3}$ .



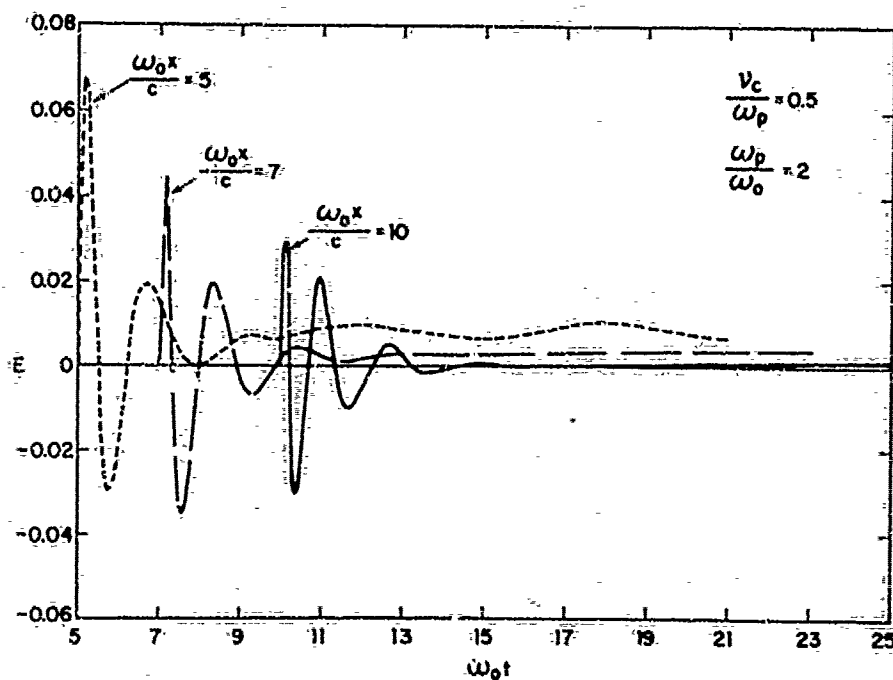


Figure 8. Transient Response to Step-Carrier Sine Wave for  $\nu_c/\omega_p = 0.5$  and  $\omega_p/\omega_o = 2$

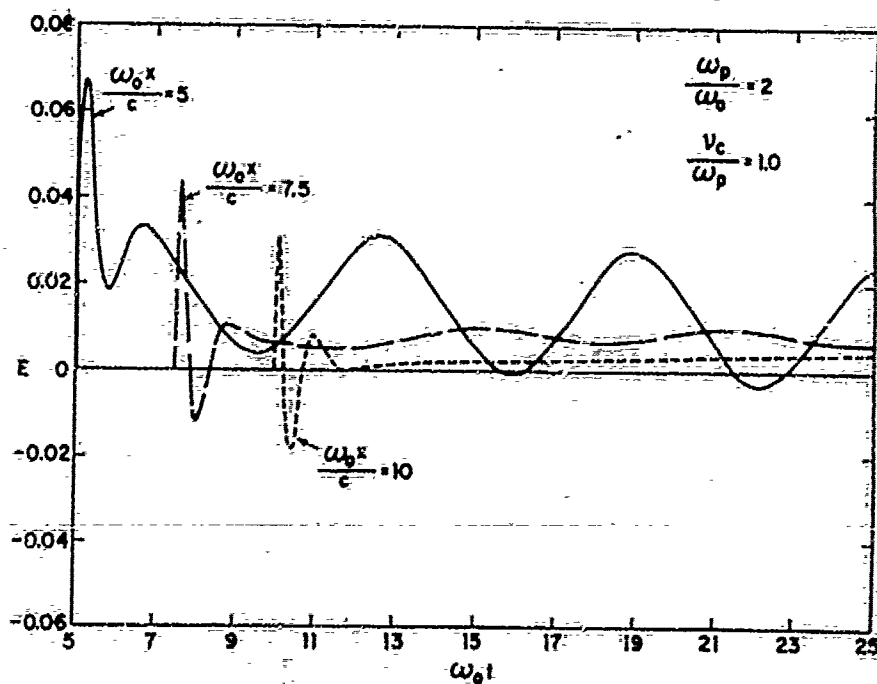


Figure 9. Transient Response to Step-Carrier Sine Wave for  $\nu_c/\omega_p = 1.0$  and  $\omega_p/\omega_o = 2$

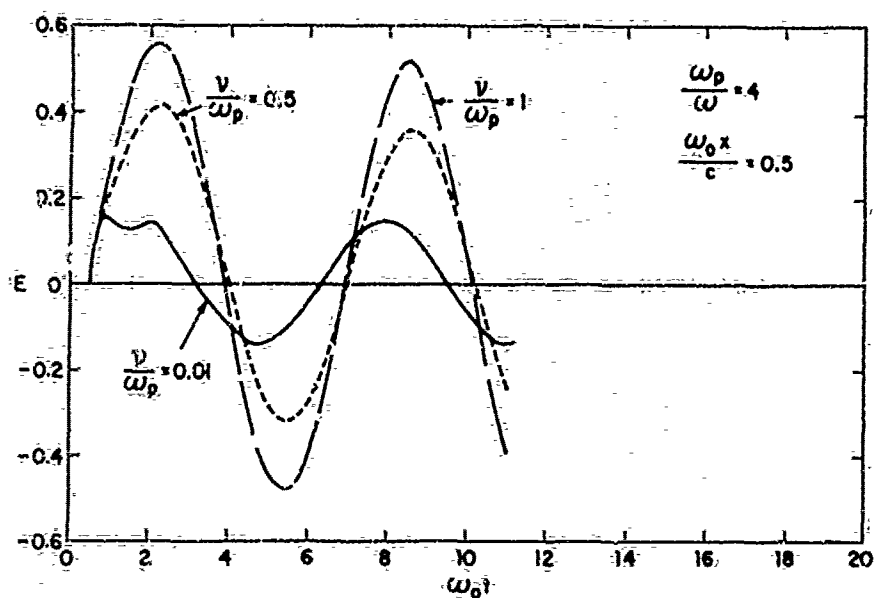


Figure 10. Transient Response to Step-Carrier Sine Wave for  $\omega_0 x/c = 0.5$  and  $\omega_p/\omega_0 = 4$

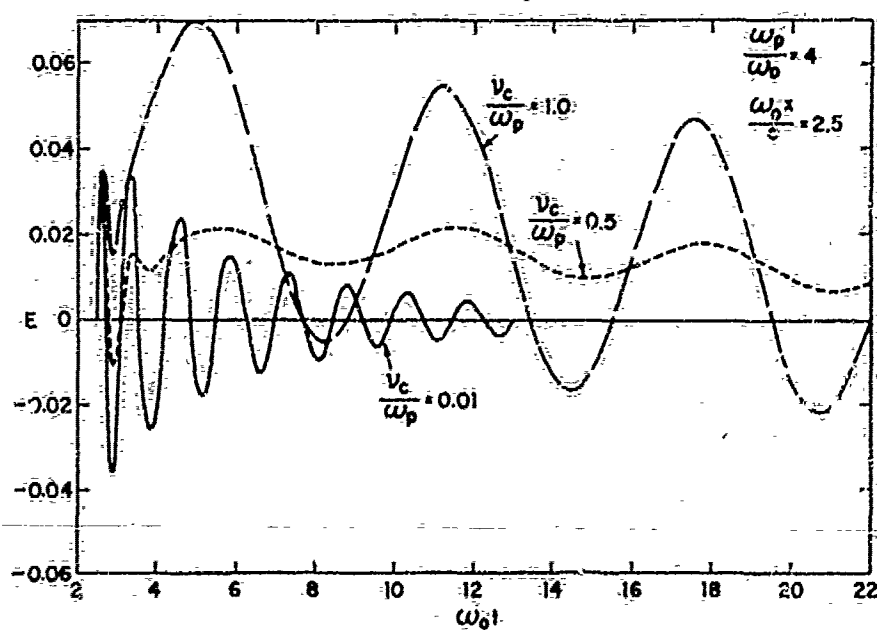


Figure 11. Transient Response to Step-Carrier Sine Wave for  $\omega_0 x/c = 2.5$  and  $\omega_p/\omega_0 = 4$

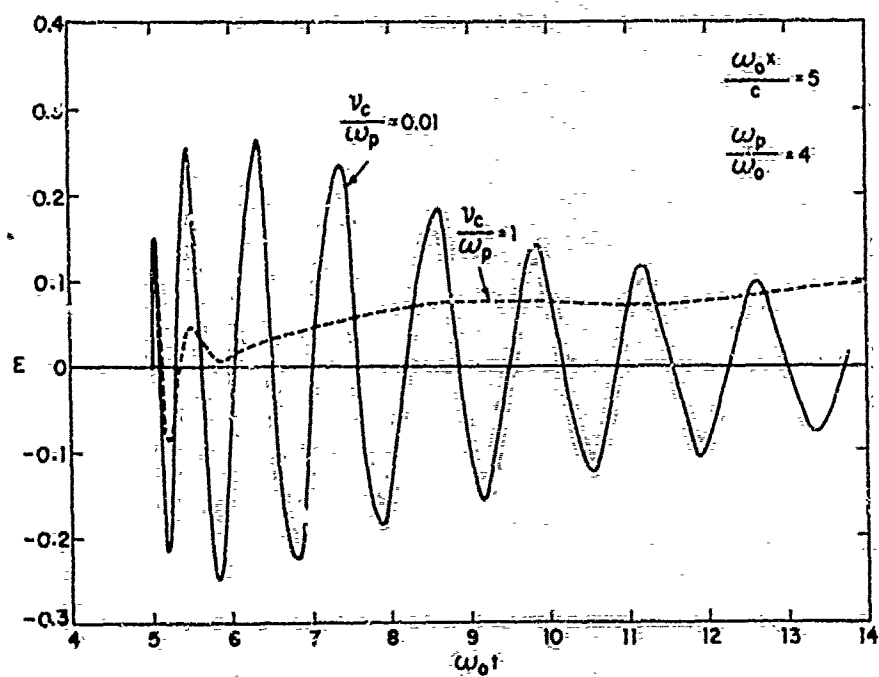


Figure 12. Transient Response to Step-Carrier Sine Wave for  $\omega_0 x/c = 5$  and  $\omega_p/\omega_0 = 4$ .

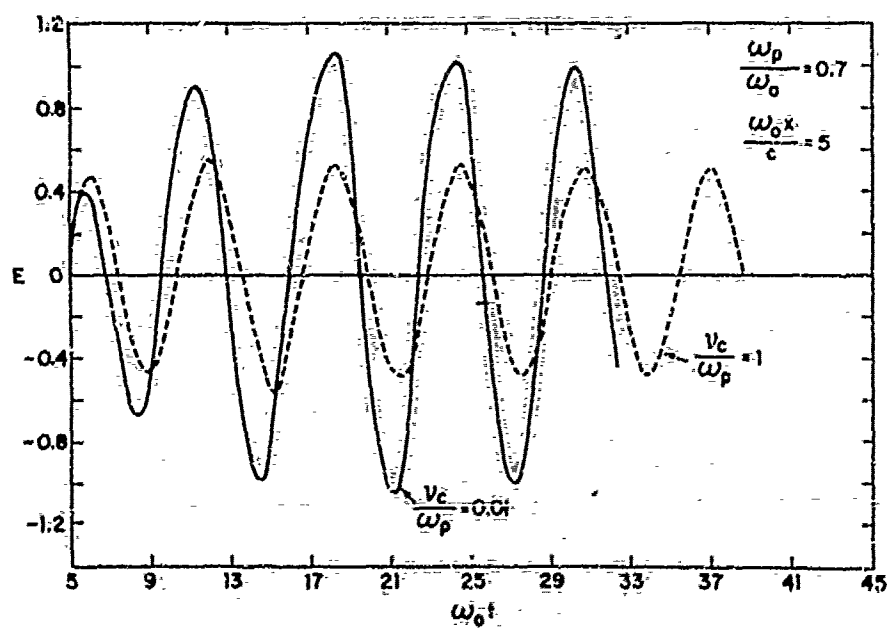


Figure 13. Transient Response to Step-Carrier Sine Wave for  $\omega_0 x/c = 5$  and  $\omega_p/\omega_0 = 0.7$ .

### 3.2 Step Function

We next consider the situation when  $E(x=0, t)$  is given by

$$E(x=0, t) = u(t) \quad (12)$$

For this case the pole  $s_0$  coincides with the branch point at  $p = 0$ , while there is no pole  $s_1$ . Here, special care must be taken in performing the integral  $I_{C_1}$ , and the integral in Eq. (7) becomes

$$I_{C_1} = I_\delta + \frac{1}{\pi} \int_\delta^{\gamma} d\sigma \hat{E}(0, -\delta) e^{-\sigma t} \sin \frac{x}{c} \left[ \left( \frac{\sigma}{\nu_c - \sigma} \right) \left( \omega_p^2 + \sigma^2 - \nu_c \sigma \right) \right]^{1/2}, \quad (13)$$

where  $I_\delta$  is the integral along a circle of radius  $\delta$  surrounding the origin in the  $p$ -plane. That is

$$I_\delta = \frac{1}{2\pi} \int_{-\pi}^{\pi} d\theta e^{\delta t \exp(i\theta)} e^{-\frac{x}{c} \gamma(p=\delta \exp(i\theta))} \quad (14)$$

Using the result of Eq. (13), plus the appropriate expression for  $I_{C_2}$  from Appendix A, we have calculated

$$E(x, t) = \int_{C_1} + \int_{C_2} \hat{E}(x=0, p) e^{(pt - \frac{x}{c} \gamma)} dp \quad (15)$$

Figures 14 and 15 show the transient responses to the unit step input at distances  $\omega_p x/c = 1$  and 5 within the plasma for  $\nu_c/\omega_p = 0.01, 0.1$ , and  $1.0$ . It is interesting and important to note, from Figure 15, that when  $\nu_c/\omega_p = 0.01$  the transient response for  $\omega_p t < 40$  is nearly identical to the results obtained by Haskell and Case (1966a) for  $\nu_c/\omega_p = 0$ . However, we now note that when  $\nu_c/\omega_p \neq 0$  the transient response does not approach zero as  $t \rightarrow \infty$  as it does for  $\nu_c/\omega_p = 0$ ; but rather approaches unity. It is clear from Figures 14 and 15 that the rate at which the transient grows towards unity is highly dependent on the collision frequency. For example, if  $\nu_c/\omega_p = 1$  we see from Figure 15 that the transient has reached a value of  $e^{-1}$  by  $\omega_p t \approx 16$ ; for  $\nu_c/\omega_p = 0.1$  the  $e^{-1}$  value occurs at  $\omega_p t \approx 160$ ; while for  $\nu_c/\omega_p = 0.01$  the signal has reached  $e^{-1}$  of its final value of unity at  $\omega_p t \approx 1600$ . Figure 16 illustrates the transient response at the larger distance  $\omega_p x/c = 10$ . The character of the response is essentially the same as for  $\omega_p x/c = 5$ , except that the rate of growth is toward the asymptotic value and

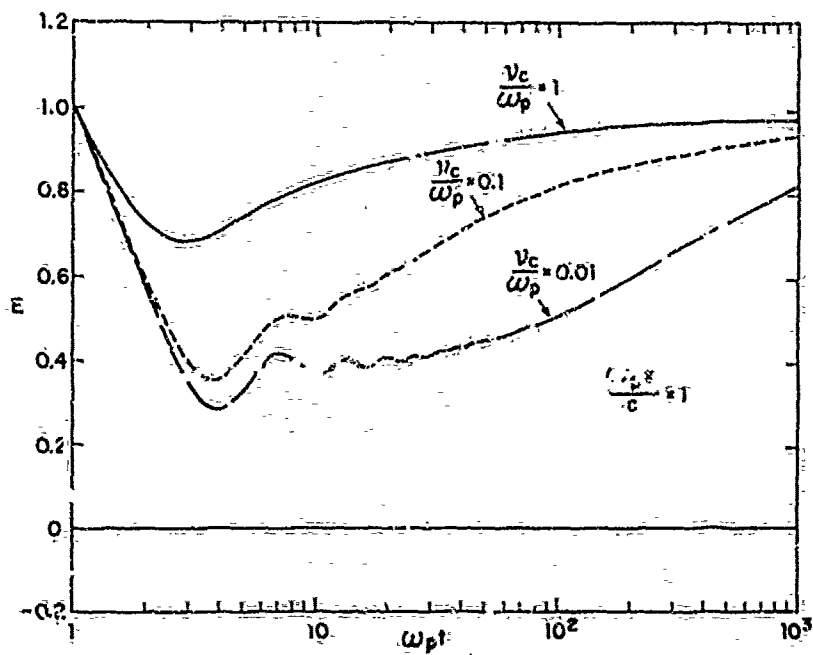


Figure 14. Transient Response to Unit Step for  $\omega_p x/c = 1$

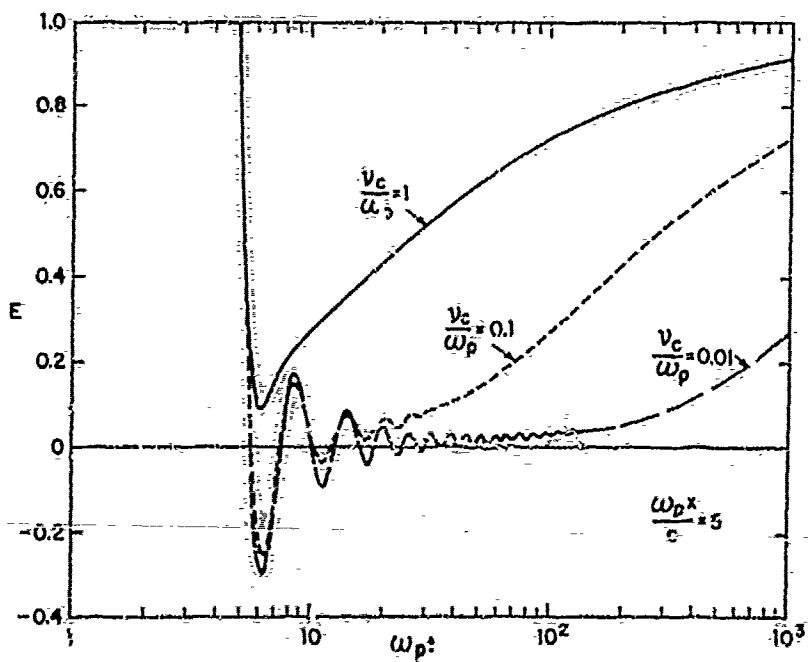


Figure 15. Transient Response to Unit Step for  $\omega_p x/c = 5$

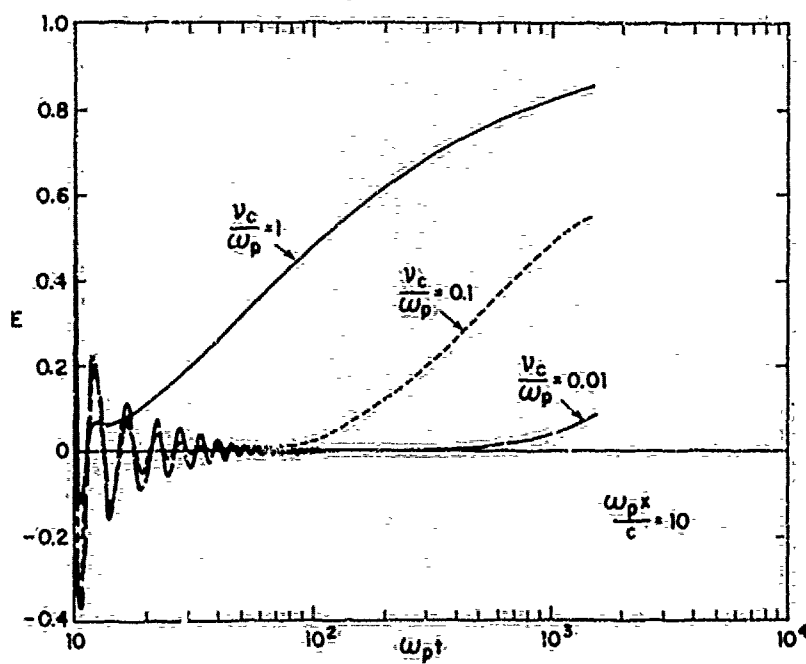


Figure 16. Transient Response to Unit Step for  $\omega_p x/c = 10$

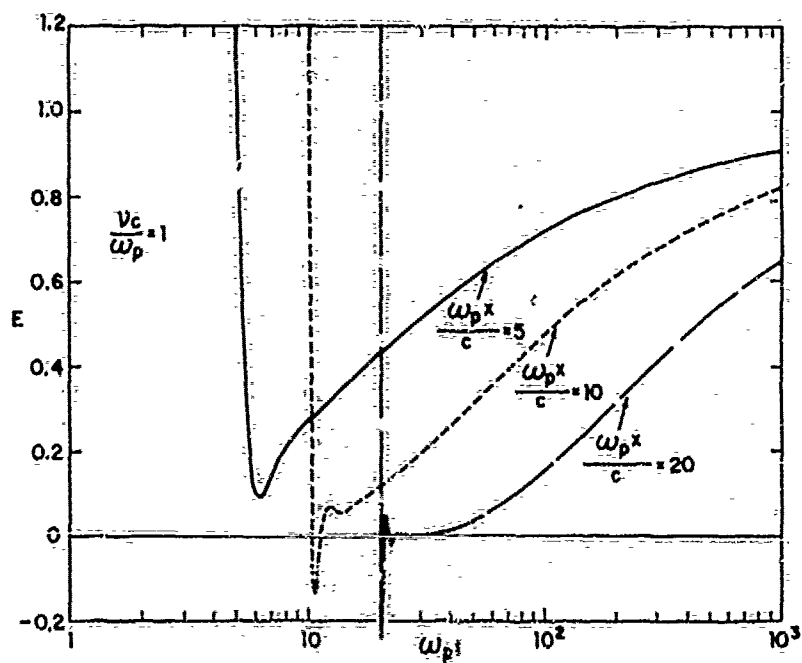


Figure 17. Transient Response to Unit Step for  $\nu_c/\omega_p = 1$

is even slower than for  $\omega_p x/c = 5$ . This point is further illustrated in Figure 17, where we compare the responses for  $\omega_p x/c = 5$ ,  $\omega_p x/c = 10$  and  $\omega_p x/c = 20$ , for the case when  $\nu_c/\omega_p = 1$ .

The behavior exhibited in Figures 14 through 17 is just what is expected physically since a wave of frequency  $\omega$  propagates as

$$\exp \left[ i \frac{\omega}{c} x \left( 1 - \frac{\omega_p^2}{\omega(\omega + i\nu_c)} \right)^{1/2} \right].$$

The behavior near the leading edge of the responses is determined by the high frequency components which propagate as  $\exp(-i\frac{\omega x}{c})$ , while the time asymptotic behavior is determined by the low frequency components, which propagate as

$$\exp \left[ x \left( \frac{i-1}{c} \right) \left( \frac{\omega_p^2 \omega}{2\nu_c} \right)^{1/2} \right],$$

which approaches unity as  $\omega \rightarrow 0$ .

It is possible to develop an accurate analytical expression for the field strength, which predicts the time asymptotic behavior we have observed in Figures 14 through 17. Let us assume that  $t \gg x/c$ ,  $\omega_p t \gg 1$ , and  $\nu_c/\omega_p$  is of order unity. Then it is shown in Appendix C that

$$E(x, t) \rightarrow 1 - \operatorname{Erf} \left[ \frac{\omega_p x}{2c(\nu_c t)^{1/2}} \right]. \quad (16)$$

This expression is quite accurate for  $t \gg x/c$  and  $\nu_c/\omega_p = o(1)$ . To illustrate this we have compared the results of Eq. (16) with the exact result in Table 1, for  $\nu_c/\omega_p = 1$  and  $\omega_p x/c = 1$  and 10. We note that the agreement is excellent once we are not too close to  $t = x/c$ . Equation (16) is not nearly so accurate for smaller values of  $\nu_c/\omega_p$  since then it is no longer legal to neglect  $\sigma$  in comparison with  $\nu_c$  in the argument of the sine function in Eq. (13). A comparison of the exact results with the approximation of Eq. (16) for  $\nu_c/\omega_p = 0.1$  is given in Table 2. As expected, the agreement is not generally good.

#### 4. DISCUSSION

The most interesting point we have noted in this report is the effect of plasma losses on the transient response of a unit step. As pointed out in Section 1, this result has important consequences for the interaction of EMP with the plasma.

Table 1. Comparison of Exact Results for the Transient E-Field With the Approximation of Eq. (16) for  $\nu_c/\omega_p = 1$

$\frac{\omega_p x}{c} = 1$			$\frac{\omega_p x}{c} = 10$		
$\omega_p t$	Eq. (16)	Exact	$\omega_p t$	Eq. (16)	Exact
1	0.480	1.0	10	0.026	1.0
3	0.682	0.685	30	0.197	0.197
5	0.753	0.740	100	0.480	0.479
10	0.823	0.823	300	0.683	0.683
30	0.897	0.897	1000	0.823	0.823
100	0.944	0.944			
300	0.967	0.967			
1000	0.982	0.982			

Table 2. Comparison of Exact Results for the Transient E-Field With the Approximation of Eq. (16) for  $\nu_c/\omega_p = 0.1$

$\frac{\omega_p x}{c} = 1$			$\frac{\omega_p x}{c} = 10$		
$\omega_p t$	Eq. (16)	Exact	$\omega_p t$	Eq. (16)	Exact
1	0.026	1.0	10	0.025	1.0
3	0.195	0.396	30	0.196	0.0062
5	0.315	0.410	100	0.480	0.0381
10	0.480	0.500	300	0.683	0.190
30	0.682	0.666	600	0.773	0.361
100	0.823	0.818	1000	0.823	0.479
300	0.897	0.896	1300	0.845	0.535
1000	0.944	0.943			



surrounding a reentry vehicle\*. For example, suppose the plasma sheath thickness  $x = 10$  cm,  $\omega_p = 1.5 \times 10^{10}$  sec<sup>-1</sup> and  $\nu_c = 1.5 \times 10^{10}$  sec<sup>-1</sup>. Then  $\nu_c/\omega_p = 1$  and  $\omega_p x/c = 5$ . Now suppose we had a square electromagnetic pulse of duration  $T_0 = 10^{-6}$  sec incident upon the plasma sheath surrounding a reentry vehicle. Then from Figure 16 it is clear that the nature of the signal present at the skin of the reentry vehicle when  $\nu_c = \omega_p$  is significantly different than for  $\nu_c = 0$ . This difference is illustrated qualitatively in Figure 18. It is possible using the results we have obtained for the unit step excitation to calculate the transient response for an actual EMP due to a nuclear blast, but in order to keep this report unclassified we have not presented this result here.

The calculation of the transient response presented here is readily extended to spatially inhomogeneous plasmas, by approximating the plasma by a series of homogeneous layers, each with different values of  $\omega_p$  and  $\nu_c$ . Then in the  $n$ th layer,  $\hat{E}(x, p)$  has the form

$$\hat{E}_n = A_n(p) e^{\gamma_n \frac{x}{c}} + B_n(p) e^{-\gamma_n \frac{x}{c}} \quad (17)$$

where  $A_n$  and  $B_n$  are obtained by requiring that  $E$  and  $\partial E/\partial x$  be continuous across the interface between each layer, and  $\gamma_n$  is given by Eq. (3) with the values of  $\omega_p$  and  $\nu_c$  in the  $n$ th layer used.

The methods used here can also be readily extended to calculate transient behavior in a lossy dielectric or in a conductor. For this case, it is readily shown that the step function response at a point  $x$  within the material is given by

$$E(x, t) = 1 - \frac{1}{\pi} \int_0^1 \frac{dy}{y} e^{-y\tau} \sin \left[ t y^{1/2} (1-y)^{1/2} \right], \quad (18)$$

where  $\tau = (\sigma_0/\epsilon)t$ ,  $l = \sigma_0 x/(\epsilon v)$ ,  $v = (\mu_0 \epsilon)^{-1/2}$ ,  $\epsilon$  is the dielectric permittivity of the material and  $\sigma_0$  its conductivity. For  $\tau \gg 1$  we obtain as an asymptotic representation for the step response

$$E(x, t) = 1 - \text{Erf} \left( \frac{l}{2\tau^{1/2}} \right), \quad (19)$$

so that in a conductor or lossy dielectric, the unit step function response at a given point in the material eventually approaches unity for large values of  $\tau$ . A plot of the transient response to a unit step in a lossy dielectric or conductor, as computed from Eq. 18, is shown in Figure 19.

\*It is of little consequence for the EMP propagation in the ionosphere since there  $\nu_c$  is so small that  $\nu_c/\omega_p \ll 1$ .

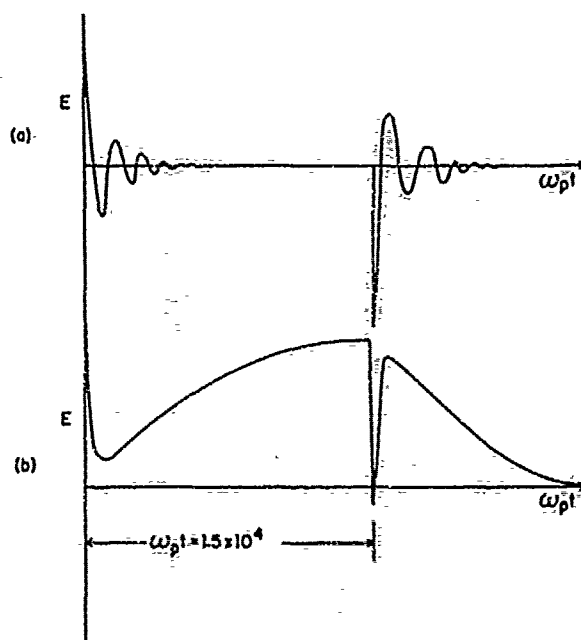


Figure 18. Response to a  $10^{-6}$  sec Square Pulse for (a)  $\nu_c = 0$ ,  $\omega_p = 1.5 \times 10^{10}$  and (b)  $\nu_c = \omega_p = 1.5 \times 10^{10}$

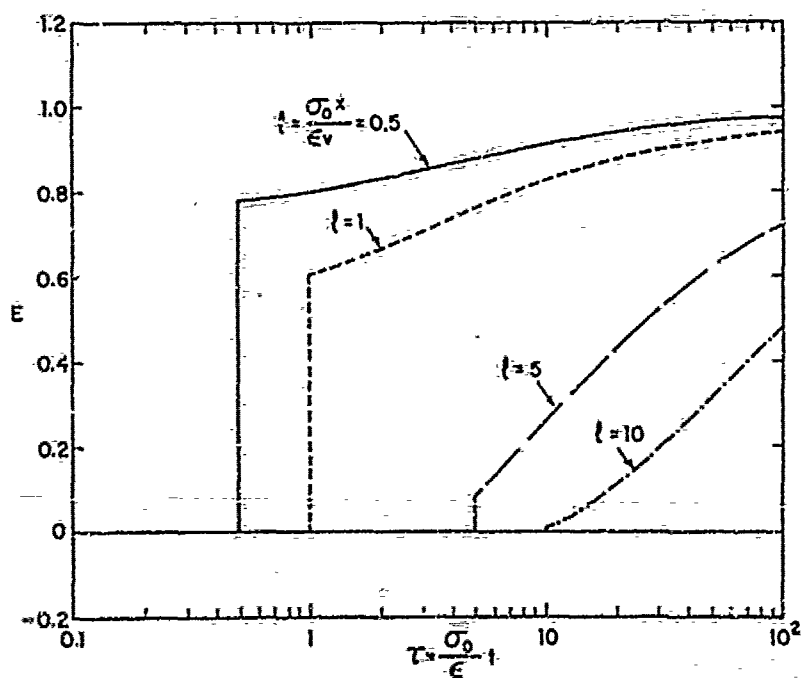


Figure 19. Transient Response of a Conductor of Lossy Dielectric to a Unit Step

## References

- Antonucci, J. (1972) An Artificial Transmission Line for Studies of Transient Propagation in Plasma Media, AFCRL-72-0055.
- Case, C. and Haskell, R. (1967) Propagation of transient signals in plasma, in Proceedings of the Symposium on the Plasma Sheath, Vol 1, edited by W. Rotman, H. Moore, R. Papa and J. Lennon, AFCRL-67-0280.
- Erdelyi, A., Magnus, W., Oberhettinger, F. and Tricomi, F. (1954) Tables of Integral Transforms, Vol 1, McGraw-Hill, New York, p. 154.
- Felsen, L. (1969) Transients in dispersive media, IEEE Trans. on Ant. and Prop. AP-17:191-200.
- Field, J. (1971) Transient Propagation of electromagnetic waves in a stratified plasma, Radio Science, 6:503-510.
- Haskell, R. and Case, C. (1966a) Transient Signal Propagation in Lossless, Isotropic Plasmas, Vol 1, AFCRL-66-234 (1).
- Haskell, R. and Case, C. (1966b) Transient Signal Propagation in Lossless, Isotropic Plasmas, Vol II, AFCRL-66-234 (2).
- Haskell, R. and Case, C. (1967) Transient signal propagation in lossless, isotropic plasmas, IEEE Trans. on Ant. and Prop. AP-15: 452-464.
- Knop, C. and Cohn, G. (1963) Comments on pulse waveform degradation due to dispersion in waveguide, IEEE Trans. on Microwave Theory and Tech. MTT-11:587-588.
- Knop, C. (1965) The transient phenomenon in an isotropic plasma without loss, Proc. IEEE 53:741-42.
- Lighthill, M. (1965) Group velocity, J. Inst. Maths. Applics 1:1-28.

## Appendix A

Here we discuss the integration along the contour  $C_2$ . Consider the point C shown in Figure 3. Here  $r_1 \equiv \rho_1 = (\eta^2 + \nu_c \eta + \omega_p^2)^{1/2}$ ,  $r_2 \equiv \rho_2 = (\eta^2 - \nu_c \eta + \omega_p^2)^{1/2}$ ,  $r_3 \equiv \rho_3 = \eta$ ,  $r_4 \equiv \rho_4 = (4\omega_p^2 - \nu_c^2 + \eta^2)^{1/2}$  and  $\theta_1 \equiv \bar{\theta}_1 = \pi/2 + \tan^{-1}[(\nu_c/2 + \eta)/Z]$ ,  $\theta_2 \equiv \bar{\theta}_2 = \tan^{-1}[Z/(\nu_c/2 - \eta)]$ ,  $\theta_3 \equiv \bar{\theta}_3 = \pi$ ,  $\theta_4 \equiv \bar{\theta}_4 = \pi/2 + \tan^{-1}(\eta/2Z)$ . At the point D, all the above quantities are the same except  $\theta_3$  which now equals  $-\pi$ . Defining  $\theta_c = 1/2(\bar{\theta}_1 - \bar{\theta}_2 + \bar{\theta}_3 + \bar{\theta}_4)$  and  $R = (\rho_1 \rho_3 \rho_4 / \rho_2)^{1/2}$ , we can then write the contour integral on the upper horizontal portion of  $C_2$  as

$$I_2' = -\frac{1}{2\pi i} \int_0^{\frac{\nu_c}{2} + \xi} d\eta e^{-\left(\eta + \frac{\nu_c}{2} - iZ\right)t} e^{\frac{x}{c} R(\cos \theta_c + i \sin \theta_c)} \hat{E}(p = -\frac{\nu_c}{2} - \eta + iZ) \\ + \frac{1}{2\pi i} \int_0^{\frac{\nu_c}{2} + \xi} d\eta e^{-\left(\eta + \frac{\nu_c}{2} + iZ\right)t} e^{\frac{x}{c} R(\cos \theta_c + i \sin \theta_c)} \hat{E}(p = -\frac{\nu_c}{2} - \eta + iZ), \quad (A1)$$

The integrals over the lower horizontal portion of  $C_2$  can be performed in a similar fashion, and yield

$$I_2'' = -\frac{1}{2\pi i} \int_0^{\frac{\nu_c}{2} + \xi} d\eta e^{-(\eta + \frac{\nu_c}{2} + iZ)t} \left[ e^{\frac{x}{c}R(\cos \theta_c - i \sin \theta_c)} - e^{-\frac{x}{c}R(\cos \theta_c - i \sin \theta_c)} \right] \hat{E}(p = -\frac{\nu_c}{2} - \eta - iZ). \quad (A2)$$

Combining Eqs. (A1) and (A2) we may write

$$I_2' + I_2'' = -\frac{e^{-\frac{\nu_c}{2}t}}{\pi} \left[ \int_0^{\frac{\nu_c}{2} + \xi} d\eta e^{-\eta t} e^{-\frac{x}{c}R \cos \theta_c} I_m \left\{ \hat{E}(p = -\frac{\nu_c}{2} - \eta + iZ) e^{i(Zt - \frac{x}{c}R \sin \theta_c)} \right\} \right. \\ \left. - \int_0^{\frac{\nu_c}{2} + \xi} d\eta e^{-\eta t} e^{\frac{x}{c}R \cos \theta_c} I_m \left\{ \hat{E}(p = -\frac{\nu_c}{2} - \eta - iZ) e^{i(Zt + \frac{x}{c}R \sin \theta_c)} \right\} \right]. \quad (A3)$$

Finally we must perform the integrals over the vertical portions of  $C_2$ . Consider the point G. At this point  $r_1 = \tilde{r}_1 = [(\nu_c + \xi)^2 + \rho^2]^{1/2}$ ,  $r_2 = \tilde{r}_2 = (\xi^2 + \rho^2)^{1/2}$ ,  $r_3 = \tilde{r}_3 = [(\nu_c/2 + \xi)^2 + (Z - \rho)^2]^{1/2}$ ,  $r_4 = \tilde{r}_4 = [(\nu_c/2 + \xi)^2 + (Z + \rho)^2]^{1/2}$ ,  $\theta_1 = \tilde{\theta}_1 = \pi - \tan^{-1}[\rho/(\nu_c + \xi)]$ ,  $\theta_2 = \tilde{\theta}_2 = \pi - \tan^{-1}[\rho/\xi]$ ,  $\theta_3 = \tilde{\theta}_3 = -\pi + \tan^{-1}[(Z - \rho)/(\frac{\nu_c}{2} + \xi)]$ ,  $\theta_4 = \tilde{\theta}_4 = \pi - \tan^{-1}[(Z + \rho)/(\frac{\nu_c}{2} + \xi)]$ .

At the point H, all the above quantities remain the same except  $\theta_3 = \pi + \tan^{-1}[(Z - \rho)/(\frac{\nu_c}{2} + \xi)]$ . Defining  $\psi_0 = \frac{1}{2}(\tilde{\theta}_1 - \tilde{\theta}_2 + \tilde{\theta}_3 + \tilde{\theta}_4)$  and  $R_0 = (\tilde{r}_1 \tilde{r}_3 \tilde{r}_4 / \tilde{r}_2)^{1/2}$ , the integrals on the vertical portion of  $C_2$  can be written as

$$I_2''' = \frac{e^{-(\nu_c + \xi)t}}{\pi} \left[ \int_0^Z d\rho e^{-\frac{x}{c}R_0 \cos \psi_0} \operatorname{Re} \left\{ \hat{E}(p = -\nu_c - \xi + i\rho) e^{i(\rho t - \frac{x}{c}R_0 \sin \psi_0)} \right\} \right. \\ \left. - \int_0^Z d\rho e^{\frac{x}{c}R_0 \cos \psi_0} \operatorname{Re} \left\{ \hat{E}(p = -\nu_c - \xi + i\rho) e^{i(\rho t + \frac{x}{c}R_0 \sin \psi_0)} \right\} \right]. \quad (A4)$$

The total integral on the contour  $C_2$  is then given by

$$I_{C_2} = I_2' + I_2'' + I_2''' \quad (A5)$$

## Appendix B

Here we outline the derivation of Eq. (11). We consider the limit when  $t \gg \frac{x}{c}$ ,  $\omega_p t \gg 1$  and  $v_c/\omega_p$  is of order unity. In this case it can be shown that the integral along the contour  $C_2$  is negligible so that

$$E(x, t) = I_{C_1} + I_{C_3} + I_{C_4}, \quad (B1)$$

where  $I_{C_1}$  is given in Eq. (7) and  $I_{C_3} + I_{C_4}$  is given in Eq. (10). Now in Eq. (7) it is clear that for  $t$  large, the principal contribution to the integral must come from  $\sigma$  near zero. Therefore  $I_{C_1}$  may be approximated by expanding the integrand in Taylor series about  $\sigma = 0$ . We get

$$\begin{aligned} I_{C_1} &\approx \frac{1}{\pi \omega_0} \int_0^{\nu_c} d\sigma e^{-\sigma t} \sin\left(\frac{\sigma}{\nu_c}\right)^{1/2} \frac{\omega_p x}{c} \\ &\approx \frac{1}{\pi \omega_0} \int_0^{\infty} d\sigma e^{-\sigma t} \sin\left[\frac{\omega_p x}{c} \left(\frac{\sigma}{\nu_c}\right)^{1/2}\right]. \end{aligned} \quad (B2)$$

The integral in Eq. (B2) is a standard Laplace Transform and yields

$$I_{C_1} \approx \frac{\omega_p}{2\omega_0 c (\nu_c \pi)^{1/2}} \left(\frac{x}{t^{3/2}}\right) \exp\left(\frac{-\omega_p^2 x^2}{4c^2 \nu_c t}\right). \quad (B3)$$

Finally, upon using Eqs. (B3) and (10) in Eq. (B1), we have

$$E(x, t) = \exp \left( -\Gamma \frac{x}{c} \cos \phi \right) \sin \left( \omega_0 t - \Gamma \frac{x}{c} \sin \phi \right) + \\ + \frac{\omega_p}{2\omega_0 c (\nu_c \pi)^{1/2}} \left( \frac{x}{t^{3/2}} \right) \exp \left( -\frac{\omega_p^2 x^2}{4c^2 \nu_c t} \right). \quad (B4)$$

## Appendix C

For a unit step when  $\nu_c/\omega_p$  is of order unity and  $t \gg x/c$  we may neglect  $IC_2$  so that the transient response is given by  $IC_1$ , which from Eq. (13) with  $\delta \rightarrow 0$  is

$$E(x, t) \approx 1 - \frac{1}{\pi} \int_0^\lambda \frac{dy}{y} e^{-yT} \sin L \left[ \frac{y}{\lambda - y} (1 + y^2 - \lambda y) \right]^{1/2}, \quad (C1)$$

where  $T = \omega_p t$ ,  $\lambda = \nu_c/\omega_p$ ,  $L = \omega_p x/c$ . When  $T \gg 1$ , it is clear that the principal contribution to the integral comes from  $y$  near zero. Expanding the integrand about  $y = 0$  and extending the range of integration to  $\infty$  then yields

$$E(x, t) \approx 1 - \frac{1}{\pi} \int_0^\infty \frac{dy}{y} e^{-yT} \sin \left( \frac{L}{\lambda^{1/2}} \right) y^{1/2}. \quad (C2)$$

The integral in Eq. (B2) is a standard Laplace transform (Erdelyi et al, 1954) and upon evaluating it, we get

$$E(x, t) \approx 1 - \operatorname{Erf} \left[ \frac{L}{2(\lambda T)^{1/2}} \right]. \quad (C3)$$



Preceding page blank

## Appendix D

Here we include a Fortran listing of the computer program used to calculate the transient response of a lossy homogeneous plasma. The program inputs are  $XL = \omega_p x/c$ ,  $AL = \nu_c/\omega_p$ ,  $OM = \omega_o/\omega_p$ ,  $D$  = the radius  $\delta$  of the contour in Eqs. (13) and (14) ( $D$  is usually set to 0.01),  $M$  = number of different values of  $T = \omega_p t$  at which calculation is to be carried out, and  $L = 1$  for a unit step input, while  $L = 2$  for a step-carrier sine wave input. The program outputs are  $E$  =  $E(x, t)$  = electric field strength,  $F$  = contribution to  $E$  from poles,  $FU$  = contribution to  $E$  from integral along  $C_1$ , and  $FUNC - FUN$  = contribution to  $E$  from integral along  $C_2$ .

```

PROGRAM RON(INPUT, OUTPUT)                                000100
REAL M2, M3, M4, N1, N2, N3, N4                          000110
COMMON AL, OM, XL, L, PI, Z0                              000120
COMMON/TERMS/TERM1, TERM1SQ, TERM2, TERM2SQ, TERM3, TERM3SQ 000130
COMMON/D/D
5 READ I3, J, AL, OM, XL, L, M                             000150
IF(AL .EQ. 0.0) STOP
10 FORMAT(4F10.4,2I4)
PRINT 20, AL, OM, XL, L                                   000170
20 FORMAT(1H1,49X,*AL = *F10.4/50X,*OM = *F10.4/50X,*XL = *F10.4/50X 000180
1,*L = *I5//9X,*T*,13X,*EE*,16X,*FF*,16X,*FU*,15X,*FUN*,15X, 000190
2*FUNC*,7X,*CP SCONDS*/)
PI = 3.14159265358979                                     000200
TERM1 = 9.0 * AL                                           000210
TERM1SQ = TERM1**2                                         000220
TERM2 = 10.0 * AL                                          000230
TERM2SQ = TERM2**2                                         000240
TERM3 = 9.5 * AL                                           000250
TERM3SQ = TERM3**2                                         000260
Z0 = SQRT(1.0 - J.25*AL**2)                                000270
F2 = SQRT(AL**2 + OM**2)                                    000280
M2 = AL / F2                                               000290
F3 = SQRT((OM - Z0)**2 + (AL / 2.0)**2)                   000300
M3 = J.5*AL / F3                                           000310
F4 = SQRT((OM + Z0)**2 + (AL / 2.0)**2)                   000320
M4 = J.5*AL / F4                                           000330
G = SQRT(OM) * SQRT(F3) * SQRT(F4) / SQRT(F2)           000340
P1 = 1.0 / SQRT(2.0)                                       000350
N1 = 1.0 / SQRT(2.0)                                       000360
P2 = SQRT(0.5*(1 - M2))                                    000370
N2 = SQRT(0.5*(1 + M2))                                    000380
P3 = SQRT(0.5*(1 + M3))                                    000390
N3 = SQRT(0.5*(1 - M3))                                    000400
P4 = SQRT(0.5*(1 - M4))                                    000410
N4 = SQRT(0.5*(1 + M4))                                    000420
CP = N1*N2*N3*N4 + N1*N4*P2*P3 - N2*N4*P1*P3 + N3*N4*P1*P2 000430
1 - N2*N3*P1*P4 + N1*N3*P2*P4 - N1*N2*P3*P4 - P1*P2*P3*P4 000450
SP = P1*N2*N3*N4 - P2*N1*N3*N4 + P3*N1*N2*N4 + P1*P2*P3*N4 000460
1 + P4*N1*N2*N3 + N1*P2*P3*P4 - N2*P1*P3*P4 + N3*P1*P2*P4 000470
DO 30 J=1,M                                               000480
XX = FLOAT(J)                                             000490
IF(XX .LE. 6.0) T = XL + J.02*(XX - 1.0)                 000500
IF(XX .GE. 7.0 .AND. XX .LE. 21.0) T = XL + 0.1 + 0.2*(XX - 6.0) 000510
IF(XX .GE. 22.0) T = XL + 3.1 + (XX - 21.0)              000520
IF(L .EQ. 1) FF = FUNC(T)                                000530
IF(L .EQ. 2) FF = EXP(-G*XL*CP) * SIN(OM*T - 3*XL*SP)     000540
FUNFU = FU(T)                                              000570
FUNFUN = FUN(T)                                           000580
FUNFUNC = FUNC(T)                                          000590
EE = FF + FUNFU - FUNFUN + FUNFUNC
OPTIME = SECOND(A)
30 PRINT 40, T, EE, FF, FUNFU, FUNFUN, FUNFUNC, OPTIME
40 FORMAT(5X,F8.3,1P,5(3X,E15.3),0P,3X,F9.3)
GO TO 5
END
*****

```

```

*****00J650
FUNCTION FU(T)000660
COMMON AL, OM, XL, L, PI, ZO000670
COMMON/TT1/TT1000690
COMMON/O/D000690
TT1 = T000690
N = 1000700
TWO = 0.0000710
GO TO (5, 6), L000720
5 H = (0.999 - 0)*AL / 2.0
FOUR = FUNK1(0*AL + H)
ENDS = FUNK1(0*AL) + FUNK1(0.999*AL)
GO TO 9000760
6 H = 0.999*AL / 2.0000770
FOUR = FUNK1(H)000780
ENDS = FUNK1(0.00001) + FUNK1(0.999*AL)000790
9 SUMO = (ENDS + 4.0*FOUR) * 4 / 3.0000800
10 H = H / 2.0000810
N = 2 * N000820
TWO = TWO + FOUR000830
FOUR = 0.0000840
Y = H000850
IF(L .EQ. 1) Y = 0*AL + H
I = 0000870
20 I = I + 1000880
FOUR = FOUR + FUNK1(Y)000890
Y = Y + H + H000900
IF(I .LT. N) GO TO 20000910
FU = (ENDS + 2.0*TWO + 4.0*FOUR) * H / 3.0000920
IF(ABS(SUMO - FU) .LT. 1.0E-6) RETURN000930
SUMO = FU000940
GO TO 10000950
END000960
*****000970
*****000980
*****000990
FUNCTION FUN(T)001000
COMMON AL, OM, XL, L, PI, ZO001010
COMMON/TT2/TT2001020
TT2 = T001030
H = 9.5*AL / 2.0001040
N = 1001050
TWO = 0.0001060
FOUR = FUNK2(H)001070
ENDS = FUNK2(0.0) + FUNK2(9.5*AL)001080
SUMO = (ENDS + 4.0*FOUR) * 4 / 3.0001090
10 H = H / 2.0001100
N = 2 * N001110
TWO = TWO + FOUR001120
FOUR = 0.0001130
Y = H001140
I = 0001150
20 I = I + 1001160
FOUR = FOUR + FUNK2(Y)001170
Y = Y + H + H001180
IF(I .LT. N) GO TO 20001190
FUN = (ENDS + 2.0*TWO + 4.0*FOUR) * H / 3.0001200
IF(ABS(SUMO - FUN) .LT. 1.0E-6) RETURN001210
SUMO = FUN001220
GO TO 10001230
END001240
*****

```

```

*****001250
FUNCTION FUNC(T)001260
COMMON AL, OM, XL, L, PI, ZO001270
COMMON/TT3/TT3001280
TT3 = T001290
H = ZO / 2.0001300
N = 1001310
TWO = 0.0001320
FOUR = FUNK3(H)001330
ENDS = FUNK3(0.0) + FUNK3(ZO)001340
SUMO = (ENDS + 4.0*FOUR) * H / 3.0001350
10 H = H / 2.0001360
N = 2 * N001370
TWO = TWO + FOUR001380
FOUR = 0.0001390
Y = H001400
I = 0001410
20 I = I + 1001420
FOUR = FOUR + FUNK3(Y)001430
Y = Y + H + H001440
IF(I .LT. N) GO TO 20001450
FUNC = (ENDS + 2.0*TWO + 4.0*FOUR) * H / 3.0001460
IF(ABS(SUMO - FUNC) .LT. 1.0E-6) RETURN001470
SUMO = FUNC001480
GO TO 10001490
END001500
*****001510
*****001520
FUNCTION FUNK1(Y)001530
COMMON AL, OM, XL, L, PI, ZO001540
COMMON/TT1/TT1001550
TERM = SIN(XL*SQRT(Y*(1.0 + Y**2 - AL*Y) / (AL - Y) ) )001560
GO TO (10, 20), L001570
10 FUNK1 = -EXP(-TT1*Y) * TERM / (PI * Y)001580
RETURN001590
20 FUNK1 = OM * EXP(-TT1*Y) * TERM / (PI * (Y**2 + OM**2) )001600
RETURN001610
END001620
*****001630
*****001640
FUNCTION FUNK2(Y)001650
COMMON AL, OM, XL, L, PI, ZO001660
COMMON/TT2/TT2001670
AA = SQRT(SQRT(4.0 - AL**2 + Y**2) )001680
AB = SQRT(SQRT(Y**2 + AL*Y + 1.0) )001690
AC = SQRT(SQRT(Y**2 - AL*Y + 1.0) )001700
R = SQRT(Y) * AA * AB / AC001710
AO = ZO / SQRT(Y**2 + 1.0 + AL*Y)001720
BO = (AL / 2.0 - Y) / SQRT(Y**2 + 1.0 - AL*Y)001730
CO = 2.0*ZO / SQRT(Y**2 + 4.0 - AL**2)001740
C1 = SQRT( ( 1.0 + AO ) / 2.0)001750
C2 = SQRT( ( 1.0 + BO ) / 2.0)001760
C3 = SQRT( ( 1.0 + CO ) / 2.0)001770
S1 = SQRT( ( 1.0 - AO ) / 2.0)001780
S2 = SQRT( ( 1.0 - BO ) / 2.0)001790
S3 = SQRT( ( 1.0 - CO ) / 2.0)001800
CT = -(C1*C2*C3 + C1*S2*S3 - C2*S1*S3 + C3*S1*S2)001810
ST = -(S1*C2*C3 - S2*C1*C3 + S3*C1*C2 + S1*S2*S3)001820

```

```

SS3 = SIN(ZO*TT2 - XL*R*ST - PI)
CC3 = COS(ZO*TT2 - XL*R*ST - PI)
SS4 = SIN(ZO*TT2 + XL*R*ST - PI)
CC4 = COS(ZO*TT2 + XL*R*ST - PI)
SS1 = SIN(ZO*TT2 - XL*R*ST - PI/2.0)
CC1 = COS(ZO*TT2 - XL*R*ST - PI/2.0)
SS2 = SIN(ZO*TT2 + XL*R*ST - PI/2.0)
CC2 = COS(ZO*TT2 + XL*R*ST - PI/2.0)
EXP1 = EXP(-XL*R*CT)
EXP2 = EXP( XL*R*CT)
EXP3 = EXP(-AL*TT2/2.0 - Y*TT2)
TERM1 = AL/2.0 + Y
GO TO (10, 20), L
10 FUNK2 = 1.0 / (PI * (1.0 + AL*Y + Y**2) ) * EXP3 *
  1*(EXP1*(ZO*SS1 - TERM1*CC1) - EXP2*(ZO*SS2 - TERM1*CC2) )
  RETURN
20 TERM2 = TERM1**2
  TERM3 = (ZO - OM)**2
  TERM4 = (ZO + OM)**2
  FUNK2 = OM / (PI*(TERM2 + TERM4)*(TERM2 + TERM4) ) * EXP3*(EXP1*
    1. ((ZO**2 - OM**2 - TERM2)*SS3 - 2.0*ZO*TERM1*CC3) - EXP2 *
    2. ((ZO**2 - OM**2 - TERM2)*SS4 - 2.0*ZO*TERM1*CC4) )
  RETURN
END
*****
*****
FUNCTION FUNK3(Y)
  REAL K1, K2, K3, K4
  COMMON AL, OM, XL, L, PI, ZO
  COMMON/TT3/TT3
  COMMON/TERMS/TERM1, TERM1SQ, TERM2, TERM2SQ, TERM3, TERM3SQ
C  TERM1 = 9.0 * AL
C  TERM1SQ = TERM1**2
C  TERM2 = 10.0 * AL
C  TERM2SQ = TERM2**2
C  TERM3 = 9.5 * AL
C  TERM3SQ = TERM3**2
  YSQ = Y**2
  BA = SQRT(SQRT((TERM2SQ + YSQ) / (TERM1SQ + YSQ) ) )
  BB = SQRT(SQRT((TERM3SQ + (ZO - Y)**2) )
  BC = SQRT(SQRT((TERM3SQ + (ZO + Y)**2) )
  R = BA * BB * BC
  A2 = TERM2 / SQRT((TERM2SQ + YSQ)
  B2 = TERM1 / SQRT((TERM1SQ + YSQ)
  C2 = TERM3 / SQRT((TERM3SQ + (ZO - Y)**2)
  D2 = TERM3 / SQRT((TERM3SQ + (ZO + Y)**2)
  K1 = SQRT( (1.0 + A2) / 2.0)
  K2 = SQRT( (1.0 + B2) / 2.0)
  K3 = SQRT( (1.0 + C2) / 2.0)
  K4 = SQRT( (1.0 + D2) / 2.0)
  T1 = SQRT( (1.0 - A2) / 2.0)
  T2 = SQRT( (1.0 - B2) / 2.0)
  T3 = SQRT( (1.0 - C2) / 2.0)
  T4 = SQRT( (1.0 - D2) / 2.0)
  CS = K1*K2*K3*K4 - K1*K4*T2*T3 + K2*K4*T1*T3 + K3*K4*T1*T2
  1 SS = - K3*K2*T1*T4 + K1*K3*T2*T4 + K1*K2*T3*T4 + T1*T2*T3*T4
  SS = - T1*K2*K3*K4 + T2*K1*K3*K4 + T3*K1*K2*K4 + T1*T2*T3*K4
  1 PQ = EXP(-TERM2 * TT3) / PI

```

```

EXP1 = EXP(-R*XL*CS)
EXP2 = EXP( R*XL*CS)
BETA = XL*R*SS
GO TO (10, 20), L
10 THETA = Y*TT3 - PI/2.0
SINH = SIN(THETA - BETA)
SINP = SIN(THETA + BETA)
COSH = COS(THETA - BETA)
COSP = COS(THETA + BETA)
FUNK3 = PQ / (TERM2SQ + YSQ) * (EXP1 * (Y*COSH + TERM2*SINH)
1 - EXP2 * (Y*COSP + TERM2*SINP) )
RETURN
20 THETA = Y*TT3 - PI
SINH = SIN(THETA - BETA)
SINP = SIN(THETA + BETA)
COSH = COS(THETA - BETA)
COSP = COS(THETA + BETA)
FUNK3 = OH*PQ / ((TERM2SQ + (Y + OH)**2)*(TERM2SQ + (Y - OH)**2)) *
1 (EXP1*(YSQ - OH**2 - TERM2SQ)*COSH + 20.0*Y*AL*SINH) -
2 EXP2*(YSQ - OH**2 - TERM2SQ)*COS + 20.0*Y*AL*SINP)
RETURN
END
C*****
C*****
FUNCTION FUNR(T)
COMMON AL, OH, XL, L, PI, ZO
COMMON/TT4/TT4
TT4 = T
H = PI / 2.0
N = 1
TWO = 0.0
FOUR = FUNP(H)
ENDS = FUNP(0.0) + FUNP(PI)
SUMO = (ENDS + 4.0*FOUR) * 4 / 3.0
10 H = H / 2.0
N = 2 * N
TWO = TWO + FOUR
FOUR = 0.0
Y = H
I = 0
20 I = I + 1
FOUR = FOUR + FUNP(Y)
Y = Y + H + H
IF(I .LT. N) GO TO 20
FUNR = (ENDS + 2.0*TWO + 4.0*FOUR) * 4 / 3.0
IF(ABS(SUMO - FUNR) .LT. 1.0E-5) RETURN
SUMO = FUNR
GO TO 10
END
C*****
C*****
FUNCTION FUNP(Y)
COMMON AL, OH, XL, L, PI, ZO
COMMON/TT4/TT4
COMMON/OZO
SINE = SIN(Y)
COSINE = COS(Y)
R02 = SQRT( (1.0 + D*COSINE)**2 + (D*SINE)**2)
R03 = SQRT( (ZO - D*AL*SINE)**2 + AL**2*(0.5 + D*COSINE)**2)
R04 = SQRT( (ZO + D*AL*SINE)**2 + AL**2*(0.5 + D*COSINE)**2)

```

```

G1 = COSINE
G2 = (1.0 + D*G1) / R02
G3 = AL * (0.5 + D*G1) / R03
G4 = AL * (0.5 + D*G1) / R04
RC1 = SQRT((1.0 + G1) / 2.0)
RC2 = SQRT((1.0 + G2) / 2.0)
RC3 = SQRT((1.0 + G3) / 2.0)
RC4 = SQRT((1.0 + G4) / 2.0)
RS1 = SQRT((1.0 - G1) / 2.0)
RS2 = SQRT((1.0 - G2) / 2.0)
RS3 = SQRT((1.0 - G3) / 2.0)
RS3 = - RS3
RS4 = SQRT((1.0 - G4) / 2.0)
ACT = RC1*RC2*RC3*RC4 + RC1*RC4*RS2*RS3 - RC2*RC4*RS1*RS3 +
1   RC3*RC4*RS1*RS2 - RS1*RS4*RC2*RC3 + RS2*RS4*RC1*RC3 -
2   RS3*RS4*RC1*RC2 - RS1*RS2*RS3*RS4
AST = RS1*RC2*RC3*RC4 - RS2*RC1*RC3*RC4 + RS3*RC1*RC2*RC4 +
1   RS1*RS2*RS3*RC4 + RC1*RC2*RC3*RS4 + RS1*RS2*RS3*RS4 -
2   RC2*RS1*RS3*RS4 + RC3*RS1*RS2*RS4
ARR = SQRT(D * R03 * R04 / R02) * XL
ARC = ARR * ACT
ARS = ARS * AST
FUNK = (1.0/PI) * EXP(D*AL*TT4 * COSINE - ARS) * COS(D*AL*TT4 * SINE - ARS)
RETURN
END

```

003050  
003060  
003070  
003080  
003090  
003100  
003110  
003120  
003130  
003140  
003150  
003160  
003170  
003180  
003200  
003210  
003240  
003250

```

03/16/73   CRL SCOPE 3.3   C00308A   02/01/72
16.25.56.TAYLXD1
16.25.56.TAYLX,CH10000,T10.
16.25.56.       7206   TAYLOR
16.25.56.NOBULL.
16.25.56.COPYSBF,INPUT,OUTPUT.
16.25.57.MASS STORAGE= 000062 PRJS
16.25.57.CP      .057 SEC.
16.25.57.PP      .518 SEC.
16.25.57.I0      .09u SEC.

```